Int. J. Heat Mass Transfer. Vol. 35, No. 12, pp. 3335–3344, 1992
Printed in Great Britain

0017–9310/92 $5.00 + 0.00
Pergamon Press Ltd

Transient forced convection in the entrance region of concentric annuli

M. A. I. EL-SHAARAWI†
King Fahd University of Petroleum and Minerals, Box No. 1893, Dhahran 31261, Saudi Arabia

and

M. K. ALKAM
Mechanical Engineering Department, Jordan University of Science and Technology, Irbid, Jordan

(*Received* 14 *June* 1991 *and in final form* 7 *February* 1992)

Abstract—The paper presents a finite-difference scheme to solve the transient laminar forced convection problem in the entry region of a concentric annulus with sumultaneously developing hydrodynamic and thermal boundary layers. Four initial conditions are considered for the creation of thermal transients. These correspond to either a step change in temperature at one of the annulus boundaries or to a simultaneous step change in temperature at both the inlet cross-section and one of the annulus boundaries, the other annulus boundary is kept adiabatic in all cases. Numerical results are presented for a fluid of $Pr = 0.7$ in an annulus of radius ratio 0.5.

INTRODUCTION

TRANSIENT forced convection heat transfer in channels is of great importance in connection with the design of control systems for modern heat exchanger devices. Other important applications which require the evaluation of the performance of thermal equipment in the unsteady forced convection regime include processes such as, start-up, shut-down, power-surge, pump-failure accidents, etc. Such processes have stimulated investigations to determine the transient thermal response of channel flows to step changes in thermal or hydrodynamic boundary conditions. On the other hand, regenerative type heat exchangers, through which hot and cold fluids pass in succession, motivated the study of periodic thermal response of channel flows to imposed cyclic variation in boundary conditions.

In spite of the importance of transient forced convection, literature on the subject is generally limited. A review of the literature reveals that only two geometries have been considered in the research works on transient laminar forced convection, namely, parallel-plate channels and circular tubes.

Early investigations [1–3] assumed the fluid temperature and velocity to be uniform across the flow cross-section. Rizika [1] analyzed the transient response of a steady compressible fluid flow through an insulated pipe subject to a step or exponential change in inlet fluid temperature. Dusinberre [2] presented an explicit finite-difference method for computing transient temperature profiles in pipes and heat exchangers. Rizika [3] considered incompressible fluid flows in a pipe and in a simple heat exchanger with a step variation in inlet fluid temperature.

Few investigators [4–7] considered cases of unsteady heat transfer with fluid velocities varying with time. Perlmutter and Siegel [4, 5] presented analytical solutions for transient heat transfer processes caused by simultaneously changing the fluid pumping pressure and either the wall temperature or the wall heat flux in parallel-plate channels. In refs. [5, 6] the fluid velocity is assumed constant over the channel cross-section (slug-flow), but can vary with time. Yang and Ou [7] considered the hydrodynamically developing flow in tubes and parallel-plate channels with the unsteady forced convection engendered by arbitrary time-dependent inlet velocity.

Other invstigators [8–20] allowed for the variation of fluid temperature across the flow cross-section but with velocity distributions which do not change with time. Either slug or fully developed velocity distributions were assumed in such investigations. Sparrow and Siegel [8] used the method of characteristics to determine the thermal response to a step change in wall temperature or wall heat flux for laminar fully developed (Poiseuille) flow in the thermal entrance region of a pipe. Their solution could be generalized to apply for arbitrary time variations by means of superposition techniques. Transient laminar heat transfer in the thermal entrance region of a parallel-plate channel subject to a step change in wall tem-

† On leave from Alazhar University, Nasr City, Cairo, Egypt.

NOMENCLATURE

C_p specific heat of fluid at constant pressure
k number of time increments in the numerical mesh network
m number of axial increments in the numerical mesh network
n number of radial increments in the numerical mesh network
N annulus radius ratio, r_1/r_2
p pressure of fluid at any point
P dimensionless pressure, $p/(\rho u_0^2)$
p_0 pressure of fluid at annulus entrance
Pr Prandtl number, ν/α
q local heat flux at the wall, $-\kappa(\partial T/\partial R)_w$
Q dimensionless wall heat flux, $(\partial\theta/\partial R)_w$
q_t total heat absorbed by fluid from entrance cross-section until a point under consideration, $2\pi\rho C_p\int_{r_1}^{r_2} ru(T_m - T_a)\,dr$
Q_t dimensionless heat absorbed by fluid, $q_t/[u_0\pi\rho C_p r_2^2(T_w - T_0)] = 2\int_N^1 RU\theta\,dR$
r radial coordinate
r_w heated wall radius
r_1 inner radius of the annulus
r_2 outer radius of the annulus
R dimensionless radial coordinate, r/r_2
Re Reynolds number, $2\rho r_2 u_0(1-N)/\mu$
t time
T temperature
T_0 fluid temperature at annulus entrance
T_{ad} adiabatic wall temperature
T_m mixing cup temperature over any cross-section, $\int_{r_1}^{r_2} urT\,dr/\int_{r_1}^{r_2} ur\,dr$
T_w heated wall temperature
u axial velocity
$\bar{u}$ average axial velocity
u_0 axial velocity at annulus entrance, $u_0 = \bar{u}$
U dimensionless axial velocity, u/u_0
U_{max} maximum dimensionless axial velocity component
v radial velocity
V dimensionless radial velocity, $r_2 v/\nu$
z axial coordinate
Z dimensionless axial coordinate, $2(1-N)z/r_2^2\,Re$.

Greek symbols

α fluid thermal diffusivity, $\kappa/\rho C_p$
θ dimensionless temperature at any point, $(T-T_0)/(T_w-T_0)$
θ_{ad} dimensionless adiabatic wall temperature, $(T_{ad}-T_0)/(T_w-T_0)$
θ_m dimensionless mixing cup temperature, $(T_m-T_0)/(T_w-T_0) = \int_N^1 RU\theta\,dR/\int_N^1 RU\,dR$
κ thermal conductivity of the fluid
μ dynamic fluid viscosity
ν kinematic fluid viscosity, μ/ρ
ρ fluid density
τ dimensionless time, vt/r^2.

perature or in wall heat flux was investigated by Siegel and Sparrow [9]. They employed the method of characteristics to solve an integral form of the energy equation with a fully developed velocity profile. Combining a transient heat conduction solution and a steady convection solution, Siegel [10] obtained a solution for transient heat transfer resulting from a step change in wall heat flux for laminar slug-flow in parallel-plate channels. Assuming fluid velocity distribution is fully developed and unchanging with time, Siegel [11] dealt with the problem of transient heat transfer in circular tubes or parallel-plate channels whose walls undergo a step change in temperature. With a uniform fluid velocity (slug-flow condition) throughout a parallel-plate channel, Siegel [12] found that the heat capacity of the plates has a very substantial effect in reducing the time response of the surface temperatures.

By means of a double Laplace transform technique, Hudson and Bankoff [13] obtained asymptotic solutions for heat transfer to a Poiseuille flow in a tube under transient conditions resulting from a step increase in wall temperature. The same technique was used by Chu and Bankoff [14] to investigate the effect of axial conduction on unsteady heat transfer to slug-flow in pipes. Their results showed that this effect is quite appreciable near the leading edge and it becomes negligible for Peclet numbers in excess of 100. Prakash [15] considered the viscous dissipation term in the energy equation and obtained an analytical solution for the unsteady temperature distribution, resulting from a step change in wall temperature, in a fully developed laminar flow inside a circular pipe. Sparrow and De Farias [16] presented results for the unsteady laminar heat transfer in a flat duct with periodically varying inlet fluid temperature and wall temperature. Again the slug-flow assumption was made. Approximate analytical solutions were obtained and compared with finite-difference solutions by Cotta and Ozisik [17] for the case of transient forced convection in fully developed laminar flow inside circular ducts and parallel-plate channels subjected to timewise variation of wall temperature.

A finite-integral-transform technique was used [18]

to obtain a solution of the case of fully developed flow between two parallel-plates with time varying inlet temperature. Lin and Shih [19] considered unsteady heat tansfer for fully developed laminar flow of power law non-Newtonian fluids in the thermal entrance region of pipes and plate slits, with viscous dissipation taken into consideration. A numerical solution to the energy equation with the axial conduction term taken into consideration was presented by Chen *et al.* [20] for the hydrodynamically fully developed flow in a pipe with a step change in wall temperature or heat flux.

To the authors' knowledge, no studies are available in the literature dealing with transient laminar forced convection in annular passages. However, of practical importance to the case under consideration is the problem of steady (with respect to time) flow in the entrance region of concentric annuli with simultaneously developing hydrodynamic and thermal boundary layers. The solution to the transient problem should asymptotically approach the steady-problem solution and hence the latter can provide a check on the transient solutions to be obtained. Such steady solutions were previously obtained by Coney and El-Shaarawi [21] and El-Shaarawi and Sarhan [22].

The lack of either theoretical or experimental data concerning the problem of unsteady laminar forced convection in annular passages, and the practical importance of this problem in the fields of nuclear reactors and double-pipe heat exchangers, motivated the present work. The present paper deals with the problem of transient laminar forced convection in the entry region of a concentric annulus. Heating starts at the entrance cross-section and thus the hydrodynamic and thermal boundary layers are developing, with respect to the space coordinates (r and z), simultaneously. However, the velocity profiles are taken to be steady with rspeect to time. Thermal transients are caused by one of the following four conditions:

(1) case (I): step change in the inner wall temperature while the outer wall is kept adiabatic ($q = 0$);

(2) case (IE): simultaneous step change in temperature at both the inner wall and the entrance cross-section, while the outer wall is kept adiabatic;

(3) case (0): step change in the outer wall temperature while the inner wall is kept adiabatic;

(4) case (OE): simultaneous step change in temperature at both the outer wall and the entrance cross-section while the inner wall is kept adiabatic.

GOVERNING EQUATIONS

Figure 1 depicits the geometry, coordinate system, and the finite-difference grid used. The fluid has constant physical properties and enters the annular passage with a uniform velocity distribution, u_0, which is unchanging in time. Prior to the start of the time-varying heating (or cooling) process, the fluid may either be in a thermal steady-state as a result of some steady heating process, or alternately, the fluid and the annulus walls may be at the same uniform temperature, T_0. The transient forced convection process starts by imposing (at $t > 0$) one of the previously mentioned four initial thermal conditions.

Assuming axisymmeric, laminar, boundary-layer flow of a Newtonian fluid, with no internal heat generation, neglecting viscous dissipation ($2\mu(\partial u/\partial z)^2$) and the axial conduction of heat ($\kappa(\partial^2 T/\partial Z^2)$), and using the dimensionless parameters given in the nomenclature, the equations of continuity, motion and energy reduce to the following non-dimensional equations, respectively

$$\frac{\partial U}{\partial Z} + \frac{1}{R}\frac{\partial (RV)}{\partial R} = 0 \tag{1}$$

$$U\frac{\partial U}{\partial Z} + V\frac{\partial U}{\partial R} = -\frac{\partial P}{\partial Z} + \frac{1}{R}\frac{\partial}{\partial R}\left(R\frac{\partial U}{\partial R}\right) \tag{2}$$

$$\frac{\partial \theta}{\partial \tau} + U\frac{\partial \theta}{\partial Z} + V\frac{\partial \theta}{\partial R} = \frac{1}{Pr}\left[\frac{1}{R}\frac{\partial}{\partial R}\left(R\frac{\partial \theta}{\partial R}\right)\right]. \tag{3}$$

It is noteworthy that the radial momentum equation has been eliminated due to the boundary-layer simplifications. However, it is possible, under the linearized numerical scheme of Bodoia and Osterle [23], to compensate for the lack of such an equation by using the following dimensionless integral continuity equation

$$\int_N^1 RU\,\mathrm{d}R = (1-N^2)/2. \tag{4}$$

Since the physical properties of the fluid are assumed constant, the equations of conservation of mass and momentum can be solved to determine the axial and radial velocity profiles (U and V), after which the energy equation can be solved using the previously obtained velocities. In the four cases considered, the initial values (at $\tau = 0$) of U, V, and θ at the boundaries are as follows:

at $Z = 0$ and $N < R < 1$:

$$U = 1 \quad \text{and} \quad V = 0;$$

for $Z > 0$ and $R = N$ or $R = 1$:

$$U = V = \theta = 0. \tag{5a}$$

The boundary conditions related to U and V for $\tau > 0$ are, for the four cases, as follows:

at $Z = 0$ and $N < R < 1$:

$$U = 1 \quad \text{and} \quad V = 0;$$

for $Z > 0$ and $R = N$ or $R = 1$:

$$U = V = 0. \tag{5b}$$

For $\tau > 0$, the thermal boundary conditions for the four cases considered are

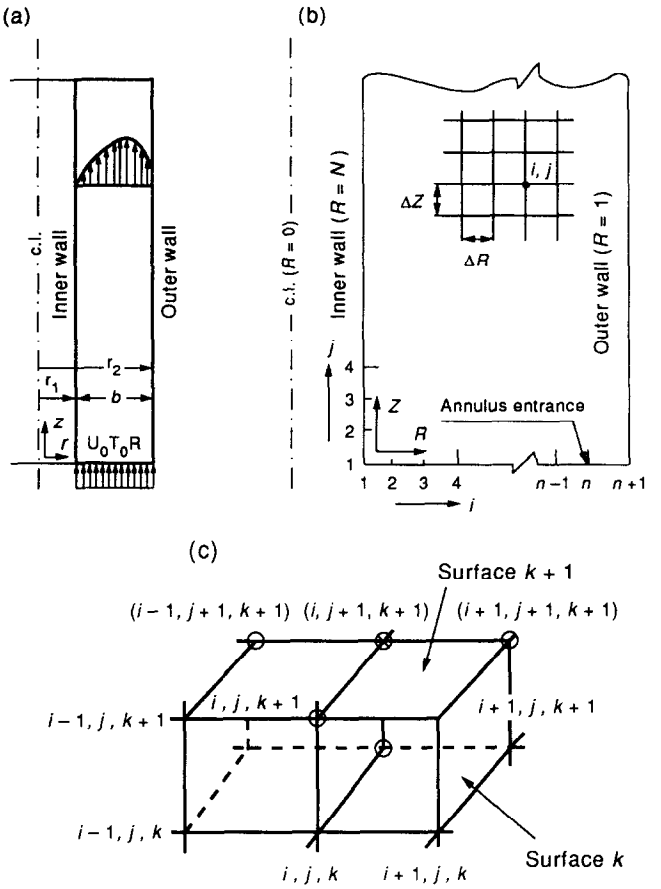

FIG. 1. Model of analysis: (a) two dimensional channel; (b) finite-difference network in R–Z plane; (c) mesh network for energy equation.

	case (I)	case (IE)
At $Z = 0$ and $N < R < 1$:	$\theta = 0$	$\theta = 1$
for $Z > 0$ and $R = N$:	$\theta = 1$	$\theta = 1$
for $Z > 0$ and $R = 1$:	$\frac{\partial \theta}{\partial R} = 0$	$\frac{\partial \theta}{\partial R} = 0$

	case (O)	case (OE)
At $Z = 0$ and $N < R < 1$:	$\theta = 0$	$\theta = 1$
for $Z > 0$ and $R = N$:	$\frac{\partial \theta}{\partial R} = 0$	$\frac{\partial \theta}{\partial R} = 0$
for $Z > 0$ and $R = 1$:	$\theta = 1$	$\theta = 1$. (5c)

NUMERICAL METHOD OF SOLUTION

In the present work, there are three independent variables; R, Z, and τ. A three-dimensional parallelpiped grid in R, Z, and τ has to be imposed on half of the annular flow field; only half of the channel is needed due to symmetry about the Z-axis. Thus, the rectangular grid shown in Fig. 1(b) is superimposed on half of the annular flow field in the R–Z plane; this grid represents the solution domain for $\tau = 0$. For other values of τ, there are other identical parallel grids, i.e. the non-dimensional time (τ) is simulated as a third coordinate normal to R–Z plane as clarified in Fig. 1(c). Mesh points are numbered consecutively from an arbitrary origin with the i progressing in the radial direction, with $i = 1$ (at the inner wall), $2, 3, \ldots,$ and $n+1$ (at the outer wall), the j progressing in the axial direction, with $j = 1$ (at inlet cross-section), $2, 3, \ldots,$ and $m+1$ (at the final arbitrary chosen cross-section), and the k progressing in the imaginary time direction, with $k = 1$ (the initial state), $2, 3, \ldots,$ and $k+1$ (at the final state). The value of m (number of steps in axial direction) is chosen such that hydrodynamic full development is ensured and the value of k is chosen such that steady-state conditions are achieved. Thus in this domain, $R_1 = N$ (inner wall), $R_{n+1} = 1$ (outer wall), $Z_1 = 0$ (channel entrance), $Z_{m+1} = L$ (channel length or height), $\tau_1 = 0$ (initial state), τ_{k+1} should be $\geqslant \tau_{ss}$ (the steady-state time). Therefore, the independent variables are designated as point functions by $R_i = N + (i-1)\Delta R$, $Z_j = (j-1)\Delta Z$, and $\tau_k = (k-1)\Delta\tau$. The dependent variables are designated as point functions with subscripts (i, j, k).

As previously stated, the velocity components U and V, due to the assumption of constant physical

properties and also the conditions imposed, are independent of time τ and temperature θ. Thus, the finite-difference equations corresponding to the continuity and momentum equations (equations (1) and (2)) can be constructed in the R–Z plane with the two dependent variables U and V having two subscripts only (i and j). Moreover, due to the boundary-layer assumptions, the pressure (P) is a function of Z only. Hence, P can have only one subscript (j). On the other hand, the three-dimensional grid depicted in Fig. 1(c) is applicable to the energy equation since the temperature is a three-dimensional function of R, Z and τ.

By an extension of the work of Bodoia and Osterle [23] equations (1), (2) and (4) can be written in the following finite-difference forms

$$\frac{V_{i+1,j+1}-V_{i,j+1}}{\Delta R}+\frac{V_{i+1,j+1}+V_{i,j+1}}{2[N+(i-\frac{1}{2})\Delta R]}+\frac{U_{i+1,j+1}+U_{i,j+1}-U_{i+1,j}-U_{i,j}}{2\Delta Z}=0 \quad (6)$$

$$V_{i,j}\frac{U_{i+i,j+1}-U_{i-1,j+1}}{2\Delta R}+U_{i,j}\frac{U_{i,j+1}-U_{i,j}}{\Delta Z}=\frac{P_j-P_{j+1}}{\Delta Z}+\frac{U_{i+1,j+1}-2U_{i,j+1}+U_{i-1,j+1}}{(\Delta R)^2}+\frac{1}{N+(i-1)\Delta R}\frac{U_{i+1,j+1}-U_{i-1,j+1}}{2\Delta R}=0 \quad (7)$$

$$2\Delta R\sum_{i=2}^{n}U_{i,j}[N+(i-1)\Delta R]=(1-N^2). \quad (8)$$

Considering the mesh network shown in Fig. 1(c), equation (3) can be written in the following finite-difference form

$$\frac{\theta_{i,j+1,k+1}-\theta_{i,j+1,k}}{\Delta\tau}+U_{i,j}\frac{\theta_{i,j+1,k+1}-\theta_{i,j,k+1}}{\Delta Z}+V_{i,j}\frac{\theta_{i+1,j+1,k+1}-\theta_{i-1,j+1,k+1}}{2\Delta R}=\frac{1}{Pr}\left[\frac{\theta_{i+1,j+1,k+1}-2\theta_{i,j+1,k+1}+\theta_{i-1,j+1,k+1}}{(\Delta R)^2}+\frac{1}{[N+(i-1)\Delta R]}\frac{\theta_{i+1,j+1,k+1}-\theta_{i-1,j+1,k+1}}{2\Delta R}\right]. \quad (9)$$

In Fig. 1(c), the circled point is the grid point under consideration and the crossed points represent those grid points involved in the difference equation (9). Also, it is shown in ref. [24] that the above finite-difference equations are consistent representations of the boundary layer equations (1)–(3) and are stable as long as the downstream axial velocity (U) is non-negative, i.e. there is no flow reversal within the domain of the solution.

The method of solving (7) and (8) to get U and P at each cross-section, after which (6) is used for the evaluation of V at the same cross-section, is discussed in ref. [23]. Now, having obtained values of U and V at a cross-section (j), equation (8) associated with the conditions (5) can be used to obtain the temperature values at $\tau+\Delta\tau$ for this particular cross-section. It is important to mention that, in equation (8) θs with subscript k are known and those with subscript $k+1$ are unknown. At each cross-section, n simultaneous linear equations have to be solved to get n temperature unknowns. The matrix of coefficients is tridiagonal and hence the Thomas method is preferred to get the solution. The same procedure is repeated for other values of j (other cross-sections) to obtain the temperature field all over the entire annulus length at $\tau+\Delta\tau$. Repeating this procedure, one can advance in time and obtain the transient temperature behaviour until steady-state conditions are practically achieved.

RESULTS AND DISCUSSION

The computations were carried out for only one value of Prandtl number, namely, 0.7, in an annulus of $N = 0.5$. Due to space limitations only a sample of the results will be presented here and detailed results may be found in ref. [24].

Figures 2–7 present examples of the developing unsteady temperature profiles at some chosen cross-sections (values of Z). Figure 2 shows the temperature profile for case (I). Hence the dimensionless temperature has a maximum value of unity at the inner isothermal wall and decreases gradually to reach its minimum value at the outer insulated wall. For case (O), Fig. 3 shows that the maximum temperature is at the outer isothermal wall. In Figs. 4–7, which are for cases (IE) and (OE), the temperature is maximum at the heated wall, after which it decreases and becomes nearly flat (has a constant value) within the

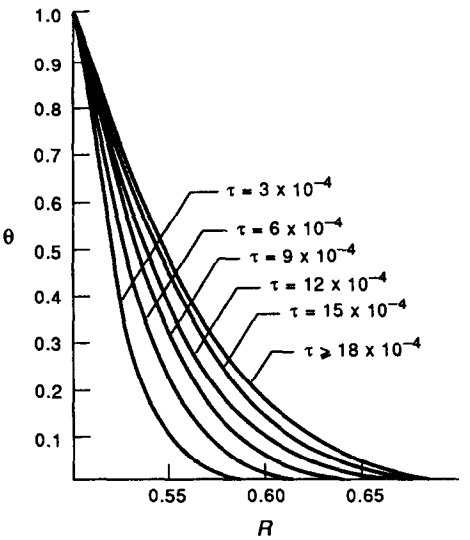

FIG. 2. Dimensionless temperature vs dimensionless radius for various values of τ, $Z = 0.003$, case (I), $N = 0.5$.

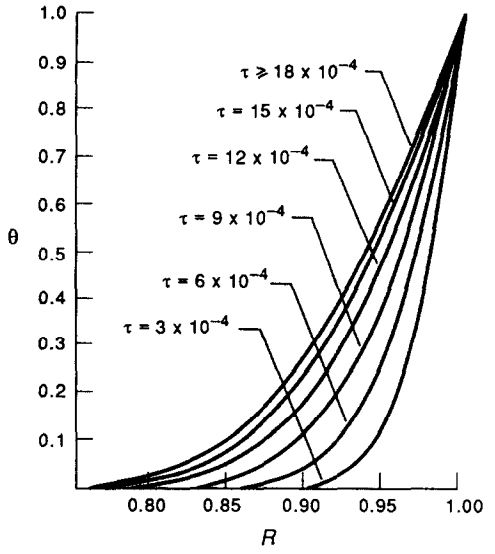

FIG. 3. Dimensionless temperature vs dimensionless radius for various values of τ, $Z = 0.0015$, case (O), $N = 0.5$.

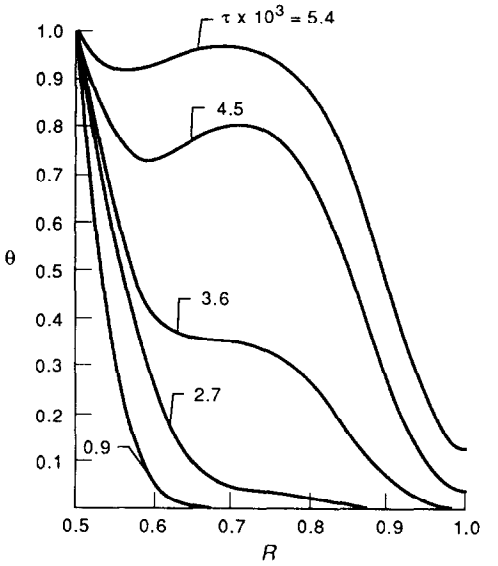

FIG. 5. Dimensionless temperature vs dimensionless radius for various values of τ, $Z = 0.005$, case (IE), $N = 0.5$.

core region, then it decreases again gradually and reaches its minimum value at the insulated boundary. In Figs. 2–7, it can be seen that, for a chosen value of Z (cross-section), and at a given value of R (except $R = R_w$), the temperature increases as τ increases.

In Figs. 5 and 7, an interesting phenomenon for cases (IE) and (OE), which is the existence of dips near the heated wall, may be observed. This may be attributed to the fact that the axial velocity component is much smaller in the dip region than in the core region. Hence, the axially convected heat from the entrance cross-section, at which a step change in temperature occurs in both cases (IE) and (OE), to the dip region is smaller than that to the core region. This makes the temperature in the core region higher than that in the region close to the heated wall.

For a given τ, Figs. 8 and 9 clarify the effect of the axial distance Z on the temperature profiles for cases (I) and (OE) respectively. Again, Fig. 8 shows that, for case (I), the closer the position to the heated wall the higher the temperature. Similarly, Fig. 9 shows that the highest temperature is always at the heated wall but the core fluid may have a higher temperature than some fluid near the heated boundary. Moreover,

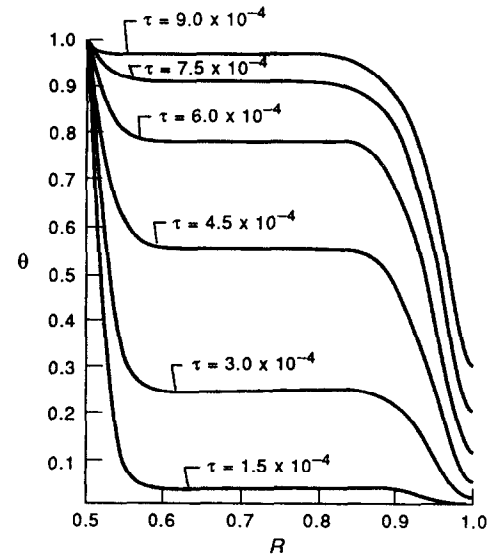

FIG. 4. Dimensionless temperature vs dimensionless radius for various values of τ, $Z = 0.0005$, case (IE), $N = 0.5$.

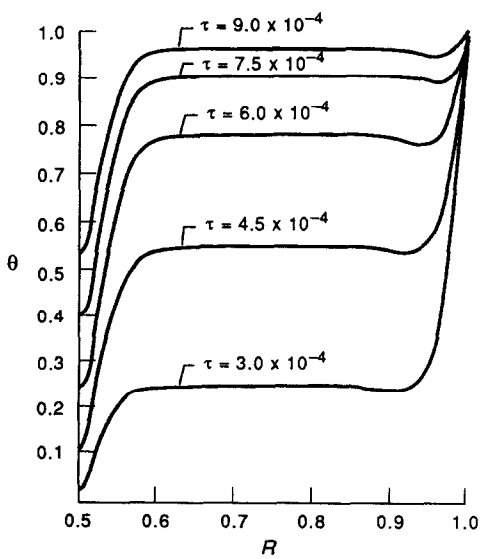

FIG. 6. Dimensionless temperature vs dimensionless radius for various values of τ, $Z = 0.0005$, case (OE), $N = 0.5$.

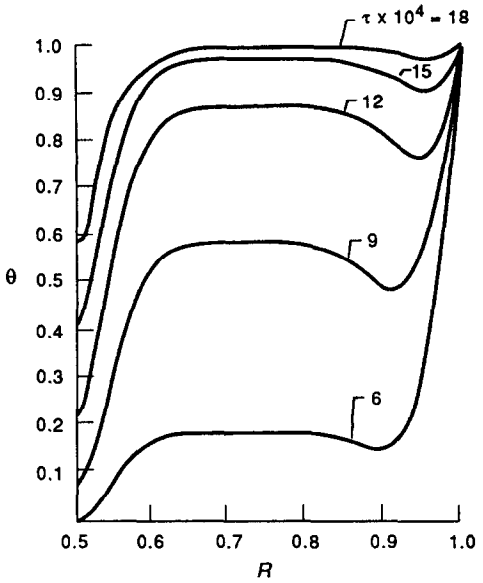

FIG. 7. Dimensionless temperature vs dimensionless radius for various values of τ, $Z = 0.001$, case (OE), $N = 0.5$.

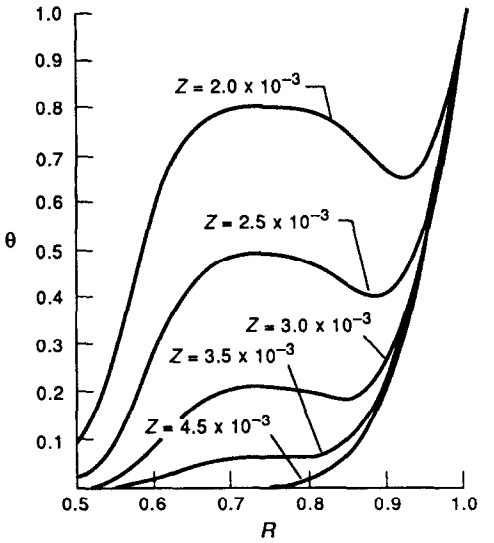

FIG. 9. Dimensionless temperature vs dimensionless radius for various values of Z, $\tau = 2 \times 10^{-3}$, case (OE), $N = 0.5$.

for a given time τ, the temperature in cases (I) and (O), is anticipated to increase as the flow moves away from the annulus entrance (i.e. Z increases). This is clarified in Fig. 8 for case (I). On the other hand, in cases (IE) and (OE), as Z increases the fluid moves away from the source of heat due to the temperature pulse at the entrance cross-section. Hence, it is expected that in cases (IE) and (OE) the temperature, for a given time, would decrease as Z increases. This is clarified in Fig. 9 for case (OE).

Engineers are not frequently concerned with the details of the fluid temperature profile but only with the mixing cup temperature. Knowing the mixing cup temperature, T_m, the total heat absorbed by the fluid (q_t) from the entrance cross-section until any distance from the entrance (Z) can be calculated. Therefore, Figs. 10 and 11 present the dimensionless mixing cup temperature (θ_m) against the dimensionless axial distance (Z) with the time τ as a parameter for the four cases considered. Figure 10, which is for cases (I) and (O), shows that, for a given value of Z and a given value of τ, θ_m in case (O) is greater than that in case (I). This can be attributed to the larger heat transfer area in case (O) than that in case (I) and hence the amount of heat absorbed by the fluid in case (O) is more than that in case (I).

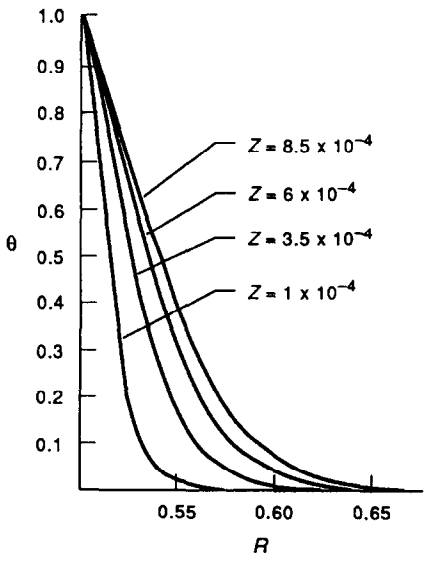

FIG. 8. Dimensionless temperature vs dimensionless radius for various values of Z, $\tau = 10^{-3}$, case (I), $N = 0.5$.

Another important observation from Fig. 10 is that, at small values of τ (early times), the mixing cup temperature reaches a maximum near the entrance (small values of Z). This phenomenon can be attributed as follows. It is known that at early times, the diffusion term (on the RHS of equation (3)) is the dominant term for the heat transfer process. In other words, at early times ($\tau < Z/U_{max}$) convection (presented by the terms containing velocity components on the LHS of equation (3)) is small compared with diffusion and the problem is very much similar to the conduction case. Also, the hydrodynamic boundary layer is known to cause the greatest resistance to the radial diffusion of heat, but its thickness is small near the entrance. Moreover, the radial velocity component V, which is responsible for transporting fluid from regions close to the heated boundary to the core region, has large values near the entrance and decays as the flow moves away from the entrance. Thus, near the entrance and at early times, there is high radial diffusion of heat beside high radial transportation of heat. These two simultaneous effects result in the

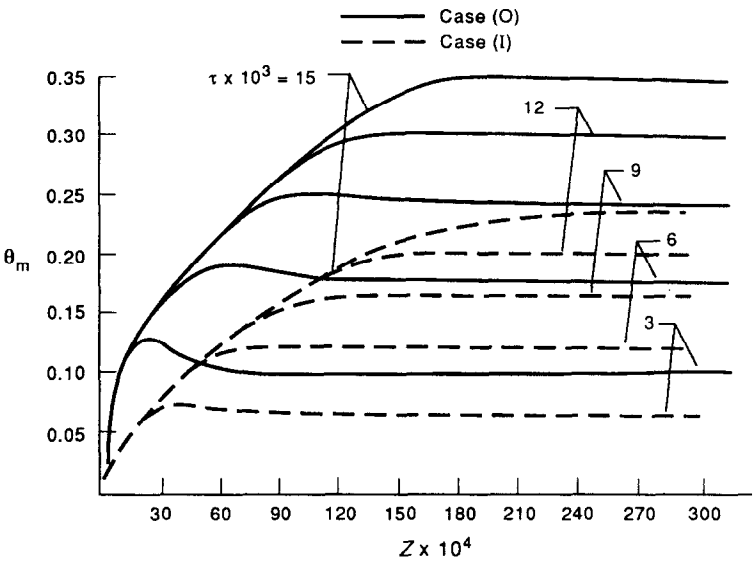

FIG. 10. Mixing cup temperature vs axial distance for various values of τ, cases (I) and (O), $N = 0.5$.

maximization of the mixing cup temperature near the entrance at early times, as shown in Fig. 10.

For cases (IE) and (OE), the behaviour of the mixing cup temperature is quite different, as shown in Fig. 11. Here, θ_m decreases monotonically with Z for all values of τ since the flow moves away from the heat pulse at the entrance. Moreover, at the same axial distance (Z) and same time (τ), θ_m for case (OE) is higher than that for case (IE). Again, this is because the heat transfer area in the former case is higher than that in the latter.

Another parameter of engineering importance is the adiabatic wall temperature (θ_{ad}). Figures 12 and 13 give the variation of θ_{ad} with τ for some chosen values of the dimensionless axial distance (Z) for the four cases investigated, i.e. cases (I), (O), (IE), and (OE). As can be seen from Fig. 12, for cases (I) and (O), θ_{ad} increases with Z and for the same axial position and time, θ_{ad} in case (O) is greater than that in case (I). On the other hand, Fig. 13 shows that, for cases (IE) and (OE), the value of θ_{ad}, at any value of τ, decreases as the fluid moves away from the entrance (i.e. Z increases). Again, θ_{ad} in case (OE) is greater, for the same Z and τ, than for case (IE).

To check the adequacy of the present results, a computer run was made with a value of N very close to unity (to approach the parallel plate channel; $N = 0.99$) and with a step temperature change at both walls. The obtained temperature profiles are presented and compared with those of Siegel and Sparrow [9] in Fig. 14 for the single value of Z at which Siegel and Sparrow [9] presented their results. Using a flat velocity profile at the entrance in the present work, the obtained temperature profiles are generally higher than those of Siegel and Sparrow [4], as shown in Fig. 14. This is expected since Siegel and Sparrow [9] assumed a fully developed flow while in the present work the flow velocity is developing and hence enhancing the convection heat transfer process. However, making another special computer run, with a

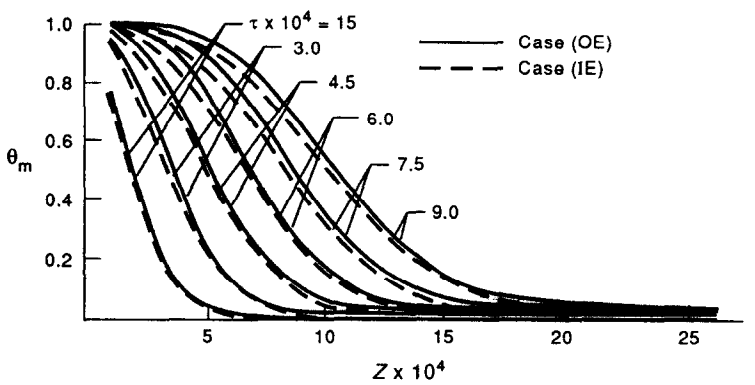

FIG. 11. Mixing cup temperature vs axial distance for various values of τ, cases (IE) and (OE), $N = 0.5$.

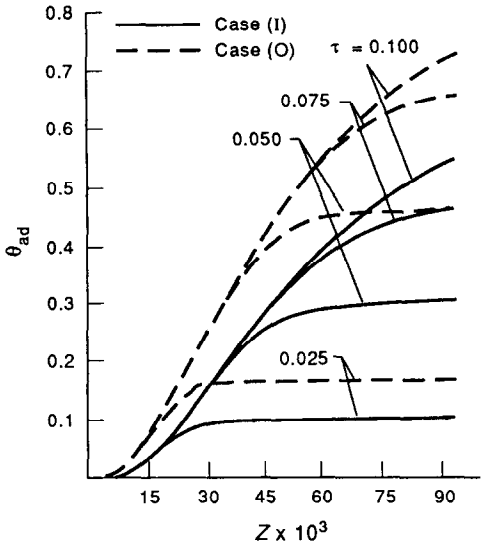

FIG. 12. Adiabatic wall temperature vs time for various values of Z, cases (I) and (O), $N = 0.5$.

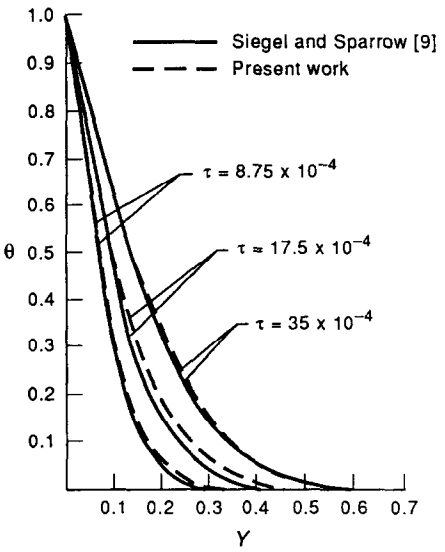

FIG. 14. Comparison of the present temperature profiles with those of Siegel and Sparrow [9], $N = 0.99$, $Z = 2.8 \times 10^{-3}$.

fully developed velocity profile right from the annulus entrance, the difference between the obtained results and those of Siegel and Sparrow [9] becomes unremarkable and the obtained temperature profiles fell on top of those of Siegel and Sparrow.

The same parallel plate channel problem was solved by Cotta and Ozisik [17] and this provides another check. Table 1 compares the obtained variation of the dimensionless wall heat flux with that of Cotta and Ozisik [17]. As can be seen from this table the present results (for $N = 0.99$) are in very good agreement with those of ref. [17] for values of $\tau \leqslant 0.05$; the maximum percentage difference is about 1.2%. However, for large value of τ (namely 0.1) the percentage difference is about 18.5%, which is relatively high. Such a large difference (at high value of τ) is due to the fact that for high values of $\tau(\tau > Z/U_{max})$ the flow is far from the conduction region in which the presented results of Cotta and Ozisik are valid.

Finally, at large values of τ, the present results have always been found to equal the steady-state results which were previously obtained in refs. [21, 22]. This provided another check on the present results.

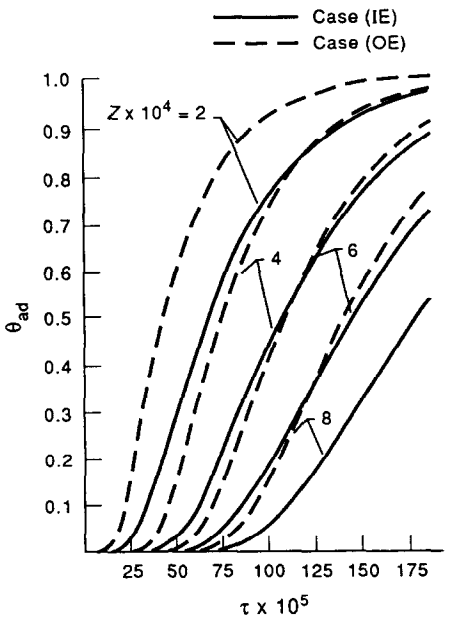

FIG. 13. Adiabatic wall temperature vs time for various values of Z, cases (IE) and (OE), $N = 0.5$.

CONCLUSIONS

A finite-difference scheme has been presented to solve the problem of transient laminar forced convection in the entry region of an annulus with simultaneously developing hydrodynamic and thermal boundary layers. Numerical results have been presented for four different initial thermal conditions. These results include the variation of the mixing cup temperature with axial distance from the entrance for various values of time. Generally, thermal responses

Table 1. Comparison of the present results with those of Cotta and Ozisik [17]

	Q	
τ	Present work	Cotta and Ozisik [17]
0.005	7.970	7.979
0.010	5.660	5.642
0.030	3.275	3.257
0.050	2.250	2.532
0.100	1.505	1.784

associated with heating the outer boundary are more pronounced than those associated with heating the inner boundary.

REFERENCES

1. J. W. Rizika, Thermal lags in flowing systems containing heat capacitors, *Trans. ASME* **76,** 411–420 (1954).
2. G. M. Dusinberre, Calculation of transient temperatures in pipes and heat exhangers by numerical methods, *Trans. ASME* **76,** 421–426 (1954).
3. J. W. Rizika, Thermal lags in flowing incompressible fluid systems containing heat capacitors, *Trans. ASME* **78,** 1407–1413 (1956).
4. H. Perlmutter and R. Siegel, Two-dimensional unsteady incompressible laminar duct flow with a step change in wall temperature, *Int. J. Heat Mass Transfer* **3,** 94–107 (1961).
5. M. Perlmutter and R. Siegel, Unsteady laminar flow in a duct with unsteady heat addition, *ASME J. Heat Transfer* **83,** 432–440 (1961).
6. R. Siegel and M. Perlmutter, Laminar heat transfer in a channel with unsteady flow and wall heating varying with position and time, *ASME J. Heat Transfer* **85,** 358–365 (1963).
7. W. Yang and J. W. Ou, Unsteady forced convection at the entrance region of closed conduits due to arbitrary time-varient inlet velocity, *JSME Semi-Int. Symposium Heat Mass Transfer*, Tokyo, Vol. 1, pp. 133–143 (1967).
8. E. M. Sparrow and R. Siegel, Thermal entrance region of a circular tube under transient heating conditions, *Proc. Third U.S. Congress for Applied Mechanics*, pp. 817–826 (1958).
9. R. Siegel and E. M. Sparrow, Transient heat transfer from laminar forced convection in the thermal entrance region of flat ducts, *ASME J. Heat Transfer* **81,** 29–36 (1959).
10. R. Siegel, Transient heat transfer for laminar slug flow in ducts, *ASME J. Appl. Mech.* **81,** 140–142 (1959).
11. R. Siegel, Heat transfer for laminar flow in ducts with arbitrary time variations in wall temperatures, *ASME J. Appl. Mech.* **82,** 241–249 (1960).
12. R. Siegel, Forced convection in a channel with wall heat capacity and with wall heating variable with axial position and time, *Int. J. Heat Mass Transfer* **6,** 607–620 (1963).
13. J. L. Hudson and S. G. Bankoff, Asymptotic solutions for the unsteady Graetz problem, *Int. J. Heat Mass Transfer* **7,** 1303–1307 (1964).
14. S. C. Chu and S. G. Bankoff, Unsteady heat transfer to slug flows: effect of axial conduction, *A.I.Ch.E. Jl* **11,** 607–612 (1965).
15. S. Prakash, An exact solution for the problem of unsteady temperature distribution in a viscous flow, *Proc. Natl. Inst. Sci. India* **A32,** 360–367 (1967).
16. E. M. Sparrow and F. N. De Farias, Unsteady heat transfer in ducts with time-varying inlet temperature and participating walls, *Int. J. Heat Mass Transfer* **11,** 837–853 (1968).
17. R. M. Cotta and M. N. Ozisik, Transient forced convection in laminar channel flow with time-wise variations of wall temperature, ASME Paper 85-WA/HT-72.
18. S. Kakac and Y. Yener, Exact solution of the transient forced convection energy equation for time-wise variation of inlet temperature, *Int. J. Heat Mass Transfer* **16,** 2205–2214 (1973).
19. H. Lin and Y. Shih, Unsteady thermal entrance heat transfer of power-law fluids in pipes and plate slits, *Int. J. Heat Mass Transfer* **24,** 1531–1539 (1981).
20. S. C. Chen, N. K. Anand and D. R. Tree, Analysis of transient laminar convective heat transfer inside a circular duct, *ASME J. Heat Transfer* **105,** 922–924 (1983).
21. J. E. R. Coney and M. A. I. El-Shaarawi, Finite-difference analysis for laminar flow heat transfer in concentric annuli with simultaneously developing hydrodynamic and thermal boundary layers, *Int. J. Numer. Meth. Engng* **9,** 17–38 (1975).
22. M. A. I. El-Shaarawi and A. Sarhan, Free convection effects on the developing laminar flow in vertical concentric annuli, *ASME J. Heat Transfer* **102,** 617–622 (1980).
23. J. R. Bodoia and J. F. Osterle, Finite-difference analysis of plane Poiseuille and Couette flow developments, *Appl. Sci. Res.* **A10,** 265–276 (1961).
24. M. K. A. Alkam, Transient forced convection in the developing region of a concentric annulus, M.Sc. Thesis, Department of Mechanical Engineering, Jordan University of Science and Technology, Irbid, Jordan (1990).